Deciphering the complex paramagnetic NMR spectra of small laccase
Dasgupta, R.

Citation
Dasgupta, R. (2021, June 15). *Deciphering the complex paramagnetic NMR spectra of small laccase*. Retrieved from https://hdl.handle.net/1887/3188356

Version:	Publisher's Version
License:	[Licence agreement concerning inclusion of doctoral thesis in the Institutional Repository of the University of Leiden](#)
Downloaded from:	[https://hdl.handle.net/1887/3188356](#)

Note: To cite this publication please use the final published version (if applicable).

Cover Page

Universiteit Leiden

The handle https://hdl.handle.net/1887/3188356 holds various files of this Leiden University dissertation.

Author: Dasgputa, R.
Title: Deciphering the complex paramagnetic NMR spectra of small laccase
Issue Date: 2021-06-15

Chapter 5

Electronic structure of the tri-nuclear copper center in the resting oxidized state for small laccase

5.1 Introduction

Laccases are multicopper oxidases that oxidize substrates and efficiently reduce oxygen to water.(1) They consist of two active sites, a type-1 (T1) copper site for oxidizing substrates and a tri-nuclear copper center (TNC) for the oxygen reduction reaction. The TNC comprises of two sites a type-3 (T3) site and a type-2 (T2) site. The T3 copper site is characterized by two coupled copper ions via a hydroxide ion and each of the Cu(II) ions are coordinated by three histidine ligands. The T2 site is characterized by a single Cu(II) ion which is coordinated by two histidine ligands and water/OH$^-$ (Figure 1.4a). Using spectroscopic techniques coupled with quantum mechanical calculations the catalytic mechanism of the oxygen reduction reaction was described for an iron oxidizing laccase Fet3p from *Saccharomyces cerevisiae* (Figure 1.3).(2) Fet3p belongs to the class of three-domain laccase where the catalytic motif of the TNC consists of the three copper ions and its coordinated imidazolyl ligands (Figure 1.4a). All ligands are thought to remain protonated throughout the catalytic cycle, which puts a positive charge bias on the entire catalytic motif. When the reaction proceeds, negative charge is accumulated, shuttled between the copper ions and the ligands, and finally transferred to oxygen.

In the two-domain laccase, the catalytic motif also has a tyrosine residue near the T2 site. This tyrosine residue was reported to take part in the oxygen reduction reaction by forming a radical during the peroxide intermediate (PI) to native intermediate (NI) conversion or during the resting oxidized (RO) state to the fully reduced (FR) state (Figure 1.3).(3–5) Although the electronic structure of the TNC for different catalytic states is defined for the three-domain laccase, this information for the two-domain laccase including the tyrosine residue is not described.

5.2 Results and discussions

The RO state of the TNC of small laccase is modelled according to the procedure described by Solomon *et al.* using the crystal structure 6s0o (chain D and E, resolution 1.80 Å; small laccase from *S. griseoflavus*) including the Tyr109 residue near the T2 site (Figure 5.1).(6, 7) In this procedure, the structure is first optimized for high, unrestricted spin, and the actual spin density is modeled in a broken symmetry single point calculation where one of the spins is flipped to match the spin state of the catalytic motif.(6, 8) Different models of the RO state were studied based on the water derived T2 site ligand and orientation of the phenolic -OH group of tyrosine (for details see Supporting Information) (Figure 5.1).

In the models where the proton of the phenolic -OH group is directed towards the water/OH⁻ ligand of the T2 site (model B and D in Figure 5.1) the T2 copper ion is reduced to Cu^{1+} with a formation of a neutral tyrosine radical. In contrast, when the proton of the phenolic -OH group is directed away (model A and C in Figure 5.1) the T2 site copper remains oxidized as Cu^{2+} and the spin density distribution is similar to that reported by Solomon *et al.* (2005, 2001) (Figure 5.1).(6, 9) Some difference in the spin density distribution at the T2 site is observed between model A and C. In model A (Figure 5.1) the electron spin density is delocalized over a copper ion and its OH⁻ ligand while in model C most of the spin density is localized on the copper ion. The spin density distribution at the T3 site is essentially the same for all the models. In model A and C, the T2 Cu^{2+} ion is a three-coordinated site with a planar geometry. It has as an open coordination oriented towards the center of the cluster with a "$d_{x^2-y^2}$" ground state (Figure 5.2). The two T3 site copper ions are antiferromagnetically coupled with each having a four-coordination environment. The T3 copper ion has the "d_{xz}" ground state while the T3' site has the "$d_{x^2-y^2}$" ground state with an open coordination directed toward the center of the cluster (Figure 5.2). These observations are consistent with experimental evidence for the RO state and previous calculations.(6, 9) The X-band EPR spectrum of the T2 site has $g_{||} > g_{\perp} > 2.00$ with large parallel hyperfine splitting suggesting a "$d_{x^2-y^2}$" ground state. While, the splitting of the absorption band at 330 nm into two-bands in the circular dichroism spectrum suggest a μ-OH bridged two Cu^{2+} ions, the characteristic feature of the T3 site.(6, 9, 10) The spin density distribution for model B and D suggests that the orientation of the proton of the phenolic -OH group of the tyrosine towards the water/OH⁻ ligand of the T2 site spontaneously leads to radical formation (Figure 5.1). In model A and C, the radical formation is not observed and this can be attributed to the distant orientation of the proton of the phenolic -OH group of the tyrosine (Figure 5.1). The energy difference between the models shows that the tyrosine radical state for models B and D is the excited state and the non-radical state in models A and C is the ground state that is relevant to describe the small laccase (Table 5.1).

5.3 Conclusion

In conclusion, the spin density distribution and geometric properties of model A and C of the RO state for small laccase is well in line with the previous report for laccase and can be considered the relevant state for the resting oxidized state of the protein under investigation, small laccase.(6) In contrast, the orientation of the phenolic -OH group from the Tyr109 residue towards the T2 site forms a tyrosine radical at higher energy. The radical formation might be an excited state that is inaccessible in the RO state. This is corroborated by experimental observations where

the radical formation is observed only after the reduction of the T3 site copper ions and the T1 site is unable to provide the next electron for the formation of a fully reduced TNC.(3, 5) This study shows that the RO state from small laccase with the tyrosine residue could be modelled and is similar to previous reports.(6) Using similar strategy other states (PI and NI) can also be modelled. It was reported that using a combination of DFT calculations and solid-state NMR spectroscopy, the resonance assignment and geometry around a single copper center can be determined with picometer resolution.(11) A similar approach can be used to assign the NMR signals reported in Chapters 2 to 4 for the RO and the NI states of small laccase. The current calculations can be used in achieving this goal.
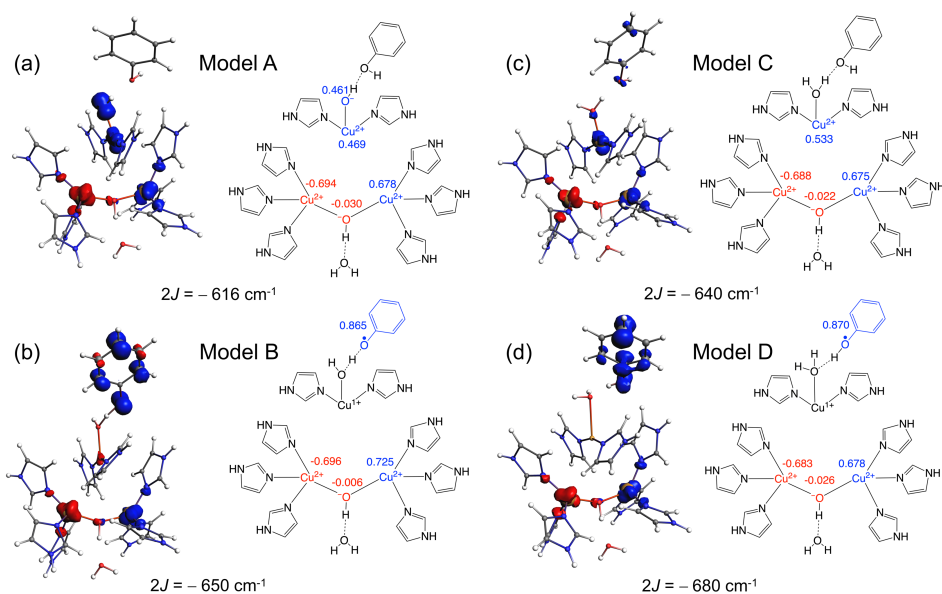

Figure 5.1. Models of the resting oxidized state based on the water / OH⁻ ligands of the T2 site and the orientation of the phenolic OH group representing the tyrosine 109 residue (from the crystal structure 6s0o, resolution 1.80 Å, organism S. greseoflavus) near the T2 site. Each panel shows the electron spin density distribution of the TNC, the schematic representation of the model with the Mulliken spin density on the three copper ions, OH⁻ ligand of the T2 site (panel a) and the phenolic group (panel b and d) and the model names. The singlet triplet energy gap (2J) is indicated below each panel. Spin densities are represented as isosurfaces. Red denotes negative phase of the spin density while blue denotes positive phase.
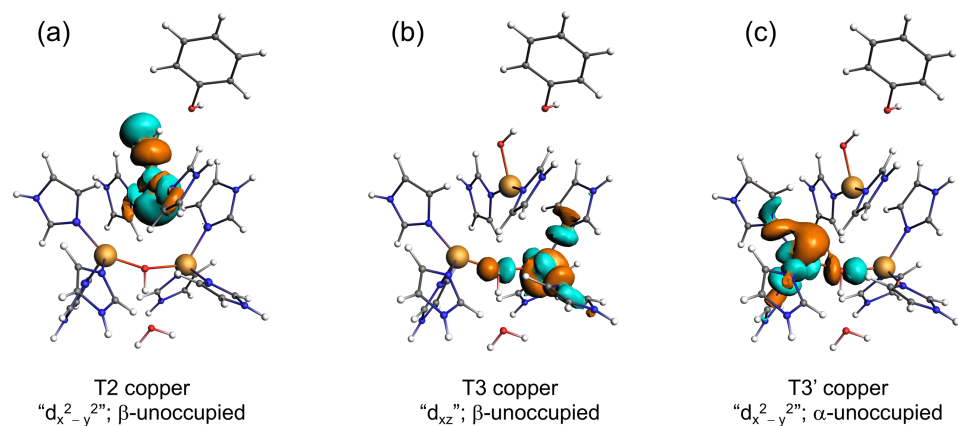
(a) T2 copper
"$d_{x^2-y^2}$"; β-unoccupied

(b) T3 copper
"d_{xz}"; β-unoccupied

(c) T3' copper
"$d_{x^2-y^2}$"; α-unoccupied

Figure 5.2. *Isosurface of α- and β-LUMOs based on the T2/T3' "$d_{x^2-y^2}$" and T3 "d_{xy}" respectively. The isosurfaces were obtained from the broken-symmetry state calculation.(6, 8)*

Table 5.1. *Energy of the high spin and broken symmetry spin state of the models of the RO state in Figure 5.1. The singlet-triplet energy gap (2J) is also shown.*

	Energy in kcal/mol			
	Model A	Model B	Model C	Model D
High Spin (HS)	-14628.220	-14615.771	-14553.125	-14551.558
Broken symmetry (BS)	-14629.100	-14616.700	-14554.040	-14552.530
Singlet-triplet gap (2J) 2(BS-HS)	-1.760 (-616 cm⁻¹)	-1.858 (-650 cm⁻¹)	-1.830 (-640 cm⁻¹)	-1.944 (-680 cm⁻¹)

5.4 Supporting Information

Model building

  The models for the RO state as shown in Figure 5.1 were built using the crystal structure 6s0o chain D and E (resolution of 1.80 Å) (7). The histidine ligands were replaced with imidazolyl and the Tyr109 (Figure 5.3) was replaced with a phenol to mimic only the side chain of these residues. The water/OH⁻ ligand of the T2 site and the bridging OH⁻ between the T3 copper ions were included. An additional conserved water molecule with a strong hydrogen bond with the bridging OH⁻ was also included. The protons were modelled using the "AddH" algorithm as implemented in the program UCSF Chimera (12). The protons at the water/OH⁻ ligand of the T2 site and the phenol were arranged as follows: model A: T2 site ligand of OH⁻ with the phenolic -OH group directed away, model B: reorientation of T2 site OH⁻ ligand in model A such that the phenolic -OH group can be directed towards it, model C: T2 site ligand of H_2O and the phenolic -OH group directed away from it and model D: reorientation of the T2 site water ligand in model C such that the phenolic -OH can be directed towards it (Figure 5.1). These models were based on the hydrogen bonding pattern of the T2 site as shown in Figure 5.3.

DFT calculation

  DFT calculations were done using Amsterdam density functional suite (13). During geometry optimization constraints were applied to reflect the crystal structure geometry of the TNC (14). The hydrogen atom replacing the side chain of the histidine ligands and the tyrosine were fixed. The dihedral angles defined by N-T3-T3'-N (T3 and T3' coppers are defined in Figure 5.1 and 5.3) were fixed to keep the eclipsed conformation. The angle of the oxygen atom from the water/OH⁻ ligand of the T2 copper relative to the histidine rings was fixed. This would prevent its artificial binding to the T3 histidine ligand. Solvent effects reflecting the protein dielectric environment was considered using conductor-like screening model as implemented in ADF suite with a dielectric constant of 4.0 (14, 15). Hybrid B3LYP (20% Hartree-Fock exchange) functional was used for all the calculations (16). A Slater-type basis set was used for all calculations (17). For geometry optimization double-ζ basis set was used for copper and nitrogen atoms while single-ζ basis set for the rest. For single-point broken-symmetry calculations the triple-ζ basis set was used for coppers and nitrogen atoms with a double-ζ basis for the rest. Broken-symmetry calculations were done by flipping the spin on the T3 copper ion (Figure 5.1).

5.5 References

1. Mano, N., and A. de Poulpiquet. 2017. O₂ Reduction in Enzymatic Biofuel Cells. *Chem. Rev.*
2. Palmer, A.E., L. Quintanar, S. Severance, T.-P. Wang, D.J. Kosman, and E.I. Solomon. 2002. Spectroscopic Characterization and O2 Reactivity of the Trinuclear Cu Cluster of Mutants of the Multicopper Oxidase Fet3p. *Biochemistry*. 41:6438–6448.
3. Gupta, A., I. Nederlof, S. Sottini, A.W.J.W. Tepper, E.J.J. Groenen, E.A.J. Thomassen, and G.W. Canters. 2012. Involvement of Tyr108 in the Enzyme Mechanism of the Small Laccase from *Streptomyces coelicolor*. *Journal of the American Chemical Society*. 134:18213–18216.
4. Tepper, A.W.J.W., S. Milikisyants, S. Sottini, E. Vijgenboom, E.J.J. Groenen, and G.W. Canters. 2009. Identification of a Radical Intermediate in the Enzymatic Reduction of Oxygen by a Small Laccase. *J. Am. Chem. Soc.* 131:11680–11682.
5. Tian, S., S.M. Jones, and E.I. Solomon. 2020. Role of a Tyrosine Radical in Human Ceruloplasmin Catalysis. *ACS Cent. Sci.*
6. Quintanar, L., J. Yoon, C.P. Aznar, A.E. Palmer, K.K. Andersson, R.D. Britt, and E.I. Solomon. 2005. Spectroscopic and Electronic Structure Studies of the Trinuclear Cu Cluster Active Site of the Multicopper Oxidase Laccase: Nature of Its Coordination Unsaturation. *J. Am. Chem. Soc.* 127:13832–13845.
7. Gabdulkhakov, A., I. Kolyadenko, O. Kostareva, A. Mikhaylina, P. Oliveira, P. Tamagnini, A. Lisov, and S. Tishchenko. 2019. Investigations of Accessibility of T2/T3 Copper Center of Two-Domain Laccase from *Streptomyces griseoflavus* Ac-993. *International Journal of Molecular Sciences*. 20:3184.
8. Onofrio, N., and J.-M. Mouesca. 2010. Valence Bond/Broken Symmetry Analysis of the Exchange Coupling Constant in Copper(II) Dimers. Ferromagnetic Contribution Exalted through Combined Ligand Topology and (Singlet) Covalent-Ionic Mixing. *J. Phys. Chem. A*. 114:6149–6156.
9. Solomon, E.I., P. Chen, M. Metz, S.-K. Lee, and A.E. Palmer. 2001. Oxygen Binding, Activation, and Reduction to Water by Copper Proteins. *Angewandte Chemie International Edition*. 40:4570–4590.
10. Solomon, E.I., U.M. Sundaram, and T.E. Machonkin. 1996. Multicopper Oxidases and Oxygenases. *Chem. Rev.* 96:2563–2606.
11. Bertarello, A., L. Benda, K.J. Sanders, A.J. Pell, M.J. Knight, V. Pelmenschikov, L. Gonnelli, I.C. Felli, M. Kaupp, L. Emsley, R. Pierattelli, and G. Pintacuda. 2020. Picometer Resolution Structure of the Coordination Sphere in the Metal-Binding Site in a Metalloprotein by NMR. *J. Am. Chem. Soc.* 142:16757–16765.
12. Pettersen, E.F., T.D. Goddard, C.C. Huang, G.S. Couch, D.M. Greenblatt, E.C. Meng, and T.E. Ferrin. 2004. UCSF Chimera—A visualization system for exploratory research and analysis. *Journal of Computational Chemistry*. 25:1605–1612.
13. Velde, G. te, F.M. Bickelhaupt, E.J. Baerends, C.F. Guerra, S.J.A. van Gisbergen, J.G. Snijders, and T. Ziegler. 2001. Chemistry with ADF. *Journal of Computational Chemistry*. 22:931–967.
14. Yoon, J., and E.I. Solomon. 2007. Electronic Structure of the Peroxy Intermediate and Its Correlation to the Native Intermediate in the Multicopper Oxidases: Insights into the Reductive Cleavage of the O−O Bond. *J. Am. Chem. Soc.* 129:13127–13136.
15. Pye, C.C., and T. Ziegler. 1999. An implementation of the conductor-like screening model of solvation within the Amsterdam density functional package. *Theoretical Chemistry Accounts: Theory, Computation, and Modeling (Theoretica Chimica Acta)*. 101:396–408.
16. Stephens, P.J., F.J. Devlin, C.F. Chabalowski, and M.J. Frisch. 1994. Ab Initio Calculation of Vibrational Absorption and Circular Dichroism Spectra Using Density Functional Force Fields. *J. Phys. Chem.* 98:11623–11627.
17. Lenthe, E.V., and E.J. Baerends. 2003. Optimized Slater-type basis sets for the elements 1–118. *Journal of Computational Chemistry*. 24:1142–1156.